
In Vivo Hemoglobin and Water Concentrations, Oxygen Saturation, and Scattering Estimates From Near-Infrared Breast Tomography Using Spectral Reconstruction¹

Subhadra Srinivasan, PhD, Brian W. Pogue, PhD, Shudong Jiang, PhD, Hamid Dehghani, PhD, Christine Kogel, RN, Sandra Soho, RN, Jennifer J. Gibson, MS, Tor D. Tosteson, ScD, Steven P. Poplack, MD, Keith D. Paulsen, PhD

Rationale and Objectives. Near-infrared (NIR) imaging has its niche in quantifying and characterizing functional changes in tissue relating to vascularity and metabolic status. Here, NIR tomography was applied to study mammographically normal breast tissue in vivo by evaluating relationships between functional parameters so obtained to clinical representers in an effort to understand factors influencing tissue compositional changes.

Materials and Methods. A new spectral reconstruction method that is considered to provide the most accurate estimates of hemoglobin level, oxygen saturation, water fraction, scattering power, and amplitude was used to assess healthy breast tissue imaged in vivo by means of NIR tomography. The approach directly recovers functional parameters with inherent inclusion of spectral behavior enforced through the incorporation of a priori model assumptions. Sixty subjects were imaged by using a frequency-domain instrument followed by spectral image reconstruction and statistical analysis for significant correlations.

Results. The new analysis shows statistically significant inverse correlations between body mass index and breast total hemoglobin and water fractions. Water fraction also correlated inversely with age and separated certain categories of breast density. Average scatter power was indicative of breast radiographic density composition, whereas scatter amplitude varied inversely with breast diameter. Total hemoglobin correlated with water fraction, whereas water correlated with scatter power.

Conclusion. The changes observed here are attributable to volume fraction alterations and provide some of the most comprehensive data on breast composition variations with demographic factors.

Key Words. Near-infrared tomography; functional imaging; breast tissue characterization; frequency-domain.

© AUR, 2006

During the past two decades, near-infrared (NIR) imaging has been developed as a way of providing functional in-

formation about the breast (1,2). Whereas current methods, such as mammography, magnetic resonance imaging, and ultrasound, provide structural and vascular data, there is a continual desire to produce imaging methods that yield new and different information about normal and diseased breast tissue. The imaging parameters in NIR tomography arise from the presence of hemoglobin, water, and lipids in tissue, which absorb light with differing spectral signatures (3,4) and relate directly to the vascular and metabolic status of the breast. In addition, elastic scattering of light is associated with the size and number density of cellular/subcellular particles that comprise the

Acad Radiol 2006; 13:195-202

¹ From the Thayer School of Engineering, Dartmouth College, 8000 Cummings Hall, Hanover, NH 03755 (S.S., B.W.P., S.J., H.D., K.D.P.); Departments of Diagnostic Radiology (C.K., S.S., S.P.P.) and Community and Family Medicine (J.J.G., T.D.T.), Dartmouth-Hitchcock Medical Center, Lebanon, NH. Received August 31, 2005; Revision received October 5; Revision accepted October 6. This work was supported through National Institutes of Health grants PO1CA80139 and U54CA105480. **Address correspondence to:** S.S. e-mail: subha@dartmouth.edu

© AUR, 2006

doi:10.1016/j.acra.2005.10.002

structural elements of breast tissue (5,6). In this study, data from 60 women with mammographically normal breasts are analyzed to determine what these NIR parameters convey about healthy breast composition as a framework for ultimately evaluating the diseased breast. The breast is a dynamic heterogeneous organ, and NIR parameters are sensitive to changes that occur with age, menstrual cycle, body mass, radiographic density, and hormonal treatment (7).

In a previous report (8), we analyzed results obtained from 24 healthy asymptomatic women to establish trends between NIR functional parameters and such clinical demographic factors as age, body mass index (BMI), breast diameter, and radiographic density. Results showed statistically significant correlations, some of which were consistent with physiological predictions (8). In this earlier investigation, the optical properties (absorption, μ_a , and reduced scattering coefficients, μ'_s) were obtained individually at each of six different wavelengths of light, and concentrations of the absorbers then were estimated by means of a spectral deconvolution procedure. Scatter parameters were determined similarly by using a spectral fit to an empirical Mie theory approximation (5,6). Since the time of the initial study, several significant improvements in algorithmic image reconstruction (9–13) have been realized that allow more accurate quantification of NIR parameters. Of particular interest has been the application of a priori information, especially of a spectral nature, that directly encodes the expected spectral behavior of the chromophore and scattering models into the image formation process (9–11). The approach implemented here uses all six wavelengths of frequency domain measurements simultaneously and incorporates Beer's law (for absorption) and Mie (for scattering) approximations that limit the solution space, as well as decrease the number of parameters to be estimated, which creates a more robust and stable algorithm. It was shown to provide improved quantification, as well as more independence of chromophore concentrations and scattering parameters (11,14).

Here, we present an expanded (to 60 subjects) evaluation of NIR imaging parameters in the healthy breast based on a more accurate direct spectral reconstruction technique. Previously reported correlations between hemoglobin and BMI and scattering and breast radiodensity remain, the new results show important statistically valid relationships with water content and decreased cross-correlation between scatter amplitude and power. These are significant findings, especially with respect

Table 1
Average and SD for Demographic and NIR Parameters From 60 Subjects With Normal Mammograms

Property	Mean \pm SD	Range
BMI (kg/m ²)	25 \pm 4	18–36
Age (y)	57 \pm 10.8	41–79
Breast diameter (mm)	80.6 \pm 13.9	49–124
Hb _T (μ M)	16.6 \pm 4.6	6–31
S _t O ₂ (%)	68.3 \pm 7.2	46–96
Water (%)	51.5 \pm 14.1	28–94
Scatter amplitude	1.2 \pm 0.25	0.59–2.2
Scatter power	0.7 \pm 0.44	0.1–3

BMI: Body mass index, Hb_T: Total hemoglobin, S_tO₂: Oxygen saturation

to water fraction, which is an important diagnostic indicator because breast cancer has greater water content (15,16).

METHODS

The NIR tomography system (17) developed at Dartmouth was used to perform all clinical breast examinations. This is a frequency-domain instrumentation designed for cross-sectional imaging of the pendent breast in an anatomically coronal configuration. Intensity-modulated light at six wavelengths in the range of 650–850 nm is used for interrogation, and amplitude and phase shift measurements of the detected light are recorded. A finite-element model of the diffusion equation represents light propagation (18), and multiwavelength data are coupled to spectral priors to recover images of total hemoglobin, oxygen saturation, water, and scatter parameters. Scatter parameters, composed of scatter amplitude (a) and scatter power (b), are estimated by enforcing the relationship $\mu'_s(\lambda) = a\lambda^{-b}$ as a constraint. Detailed derivations of the image reconstruction algorithm can be found elsewhere (11).

Informed consent was obtained from all participants, and the examination protocol was approved by the requisite institutional committee. Breast examinations were delivered under health professional supervision to ensure comfort, and pressure sensors were placed appropriately to ensure minimum pressure and a noncompressive state to minimize interference with vasculature. Optical data from each examination were calibrated and used to reconstruct for the functional images. Artifacts sometimes are found near the boundary; hence, the imaging field evalu-

Table 2
Estimated Partial Correlations With SE of NIR Parameters Relative to Such Demographic Factors as Age, BMI, and Breast Diameter

NIR Parameter	Subject Parameter	Coefficient (SE)	F P
Hb _T	Age	-0.04 (0.03)	.27
Hb _T	BMI	-0.47 (0.12)	<.001*
Hb _T	Breast diameter	-0.06 (0.03)	.064
S _t O ₂ (%)	Age	-0.07 (0.06)	.25
S _t O ₂ (%)	BMI	-0.54 (0.21)	.012*
S _t O ₂ (%)	Breast diameter	0.16 (0.06)	.006*
Water (%)	Age	-0.45 (0.10)	<.001*
Water (%)	BMI	-0.95 (0.33)	.005*
Water (%)	Breast diameter	-0.15 (0.09)	.1
Scatter amplitude	Age	0.002 (0.002)	.28
Scatter amplitude	BMI	0.009 (0.007)	.18
Scatter amplitude	Breast diameter	-0.010 (0.002)	<.001*
Scatter power	Age	-0.010 (0.003)	.005*
Scatter power	BMI	-0.009 (0.011)	.44
Scatter power	Breast diameter	-0.004 (0.003)	.19

*P-value <0.05 indicates a statistically significant relationship. BMI: Body mass index, Hb_T: Total hemoglobin, S_tO₂: Oxygen saturation

ated was reduced by 12% of the total breast diameter for each cross-section to compute the breast average and SD. Statistical analysis of these data was completed by using a standard random coefficients regression model to allow examination of the correlation and significance level for each parameter association.

RESULTS

Patient Imaging and Demographic Information

The average with SD and total range for the five NIR parameters, along with clinical data (BMI, age, and breast diameter), are listed in Table 1 for the 60 subjects imaged, 56 of whom participated in bilateral left and right breast examinations.

Correlations Between Functional Parameters and Demographic Factors

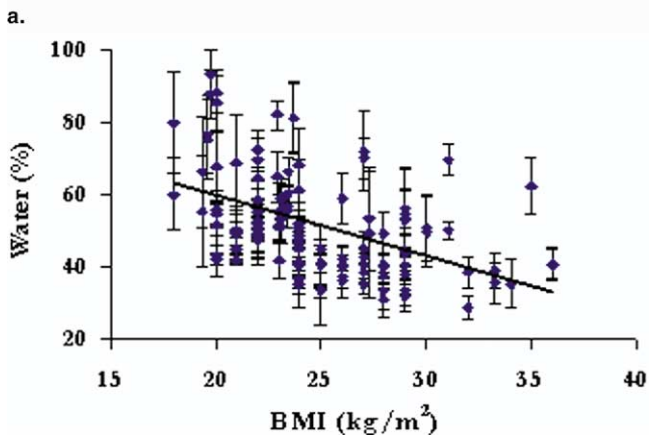
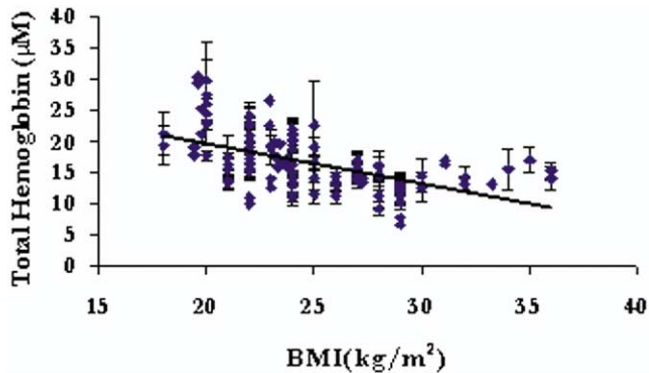
A random-coefficients regression model was used to test for relationships between each of the NIR functional parameters with clinical data (using both left and right breast results). A previous study (19) indicated a high degree of correlation between NIR parameters for the left and right breasts, and this was taken into account by appropriate model adjustment for the cross-correlation between results. Coefficients, along with SE and

P, are listed in Table 2. *P* < .05 indicates a statistically significant difference from a slope of zero for the fit between the clinical parameter (*x*) and functional property (*y*).

Total hemoglobin (Hb_T) was found to have a moderate, but highly statistically significant, negative correlation ($\rho = -0.47$) with BMI (*P* < .001). Figure 1a shows this relationship in a cluster plot of total hemoglobin averages with their respective SDs plotted against BMI for all subjects. The analysis also indicates that oxygen saturation has a moderate negative ($\rho = -0.54$) to small positive ($\rho = 0.16$), but statistically significant, relationship with BMI (*P* = .012) and breast diameter (*P* = .006), respectively. Water has a moderate ($\rho = -0.45$) to strong ($\rho = -0.95$) association with age and BMI, both highly significant statistically. Figure 1b shows the water-BMI relationship in graphical form. Scatter amplitude and power correlate with different factors: amplitude with breast diameter and scatter power with age. These relationships are plotted in Figure 2a and b, respectively.

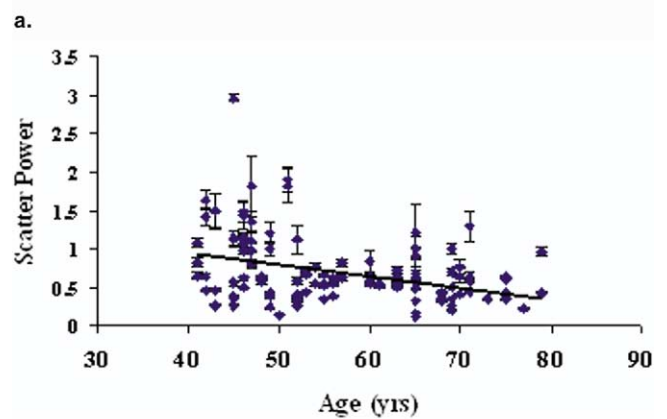
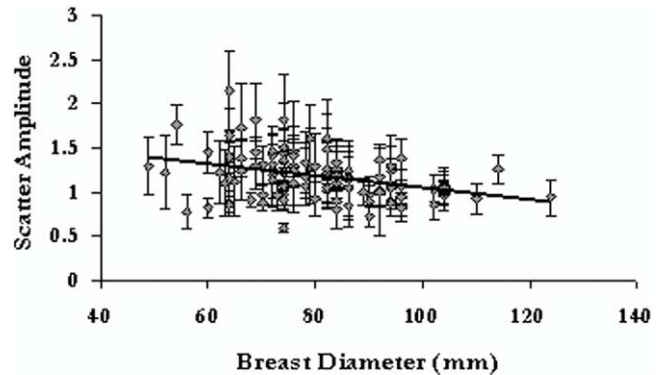
Correlations Between Functional Parameters and Radiographic Density

Another subject characteristic of considerable importance is radiographic breast composition. This is determined from the x-ray mammogram and has been classi-



b.

Figure 1. (a) Total hemoglobin and (b) water percentage plotted against BMI using data from the breasts of 60 healthy subjects. Both relationships show a statistically significant correlation ([a] $P < .001$; [b] $P = .005$).



b.

Figure 2. (a) Scatter amplitude versus diameter and (b) scatter power versus age for the same subject group in Figure 1. Both correlations are statistically significant; $P < .001$ and $P < .005$, respectively.

fied in one of four categories (20,21): (1) almost entirely fat, (2) scattered fibroglandular densities, (3) heterogeneously dense, and (4) extremely dense. Functional NIR parameters were tested for correlations with each of the radiodensity groups in a random coefficients regression model. Table 3 lists these results in a format similar to Table 2.

It appears that oxygen saturation can discriminate heterogeneously dense and extremely dense breasts from their fatty counterparts with $P = .038$ and $P = .035$, respectively. Scatter power also is statistically different across these radiodensity categories. Figure 3a shows this relationship in graphical form. In addition to the analysis listed in Table 3, we found that water could separate heterogeneously dense and extremely dense breasts from subjects with scattered radiodensity with $P = .03$ and $P = .005$, respectively. The relationship is shown in Figure 3b; it is clear that water content averages for fatty and

scattered type breasts are similar, but different statistically from heterogeneously dense and extremely dense averages. Scatter amplitude separated heterogeneously dense from scattered breasts ($P = .008$), whereas scatter power separated both heterogeneously dense and extremely dense breasts from the scattered category ($P < .001$ and $P < .001$, respectively).

Correlations Between Functional Parameters

To test for correlations between NIR parameters themselves to assess the degree of independent information obtained, a multivariate calculation of Pearson correlation coefficient was performed. Results are listed in Table 4, in which correlation coefficients are listed with the corresponding P . Hb_T appears to correlate with water (Figure 4a), and scatter power (Figure 4b), with modest linearity ($P < .001$ for both). Water also correlated with scatter power with a stronger level of linearity ($P < .001$). Scat-

Table 3
Statistical Analysis Testing of Relationships Between Radiographic Density and NIR Parameters

NIR Parameters	Radiodensity Groups	Coefficient (SE)	t-Test P
Hb _T (μmol/Lr)	Fatty	Reference	
	Scattered	-0.95 (1.22)	.44
	Het dense	-0.16 (1.30)	.9
	Extr dense	1.10 (1.76)	.53
S _t O ₂ (%)	Fatty	Reference	
	Scattered	-2.32 (2.23)	.3
	Het dense	-5.00 (2.38)	.038
	Extr dense	-6.89 (3.23)	.035
Water (%)	Fatty	Reference	
	Scattered	-3.80 (3.45)	.27
	Het dense	1.69 (3.67)	.65
	Extr dense	8.13 (4.98)	.11
Scatter amplitude	Fatty	Reference	
	Scattered	0.014 (0.073)	.85
	Het dense	-0.130 (0.078)	.1
	Extr dense	-0.023 (0.106)	.82
Scatter power	Fatty	Reference	
	Scattered	0.011 (0.117)	.92
	Het dense	0.33 (0.12)	.01
	Extr dense	0.47 (0.17)	.006

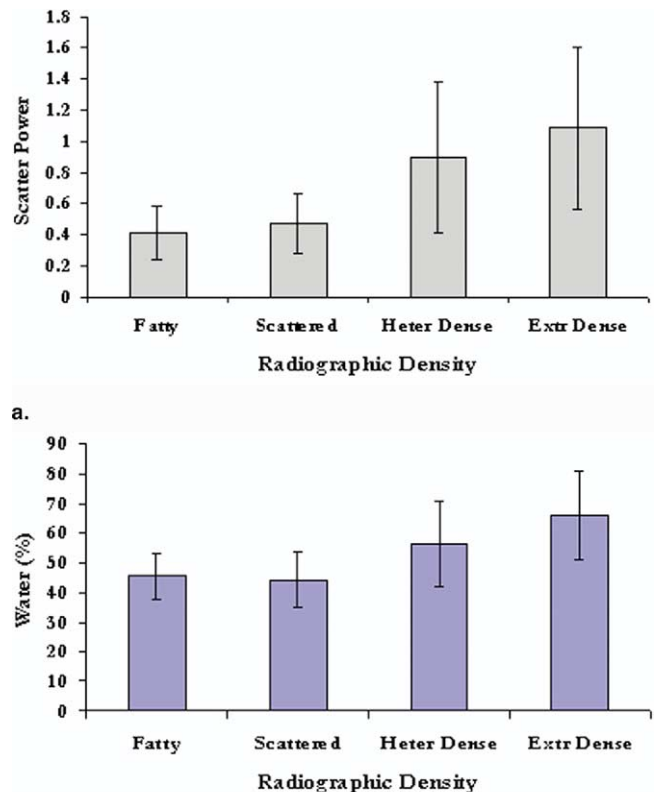
Hb_T: Total hemoglobin, S_tO₂: Oxygen saturation, Het: Heterogeneously, Extr: Extremely

ter amplitude and power correlate with each other, as expected, because both are estimated from spectral constraints introduced through an empirical approximation to Mie theory.

DISCUSSION

Studies of healthy breast tissue offer insight into the relationships between clinical factors and the functional information available through NIR imaging. The new spectral reconstruction technique allows improved quantification, along with decreased SD (<5% overall compared with higher levels of 24% for the previous approach, in experimental phantom data), which is especially significant for such parameters as water and scatter, indicated by homogeneous and heterogeneous experiments (11,14). Some of the correlations reported here are consistent with our earlier study; however, new relationships, primarily involving water and scatter, are now evident that are consistent with the improved quantification of these parameters.

Our previous study (8) showed that the clinical parameters age, BMI, and breast diameter themselves cor-



b.

Figure 3. (a) NIR scatter power as a function of radiographic density in which overall average for subjects in each category is graphed with the SD. Statistical analysis shows that scatter power can separate fatty from heterogeneously dense and extremely dense breasts from the fatty category with $P = .01$ and $P = .006$. (b) Water as a function of radiographic density. Water separates scattered from heterogeneously dense and extremely dense categories statistically with $P = .03$ and $P = .005$, respectively.

related statistically with modest linearity, suggesting that they do not yield much independent information. However, when correlating NIR parameters to these factors, we observe significant correlations to specific clinical parameters, yielding the hypothesis that each of these parameters provides information unique to the composition of the breast (e.g., Hb_T correlated with BMI, but not radiographic density). At the six wavelengths used for imaging, the contribution from lipids was found to be negligible (21); hence, lipids were not included in this data analysis. Use of wavelengths beyond 900 nm will allow us to capture some stronger features of lipids, and this is planned in future system developments. We also excluded dependence of NIR parameters on menstrual cycle, based on an earlier

Table 4
Pearson Correlation Coefficients Among Derived NIR Properties With Corresponding *P*

	Hb _T	S _t O ₂ (%)	Water (%)	Scatter Power	Scatter Amplitude
Hb _T (μmol/L)	1	0.237 (<i>P</i> = .068)	0.569 (<i>P</i> < .001)	0.494 (<i>P</i> < .001)	-0.117 (<i>P</i> = .37)
S _t O ₂ (%)		1	-0.079 (<i>P</i> = .55)	0.094 (<i>P</i> = .47)	-0.184 (<i>P</i> = .16)
Water fraction			1	0.743 (<i>P</i> < .001)	-0.235 (<i>P</i> = .071)
Scatter power				1	0.468 (<i>P</i> = .0002)
Scatter amplitude					1

Hb_T: Total hemoglobin, S_tO₂: Oxygen saturation

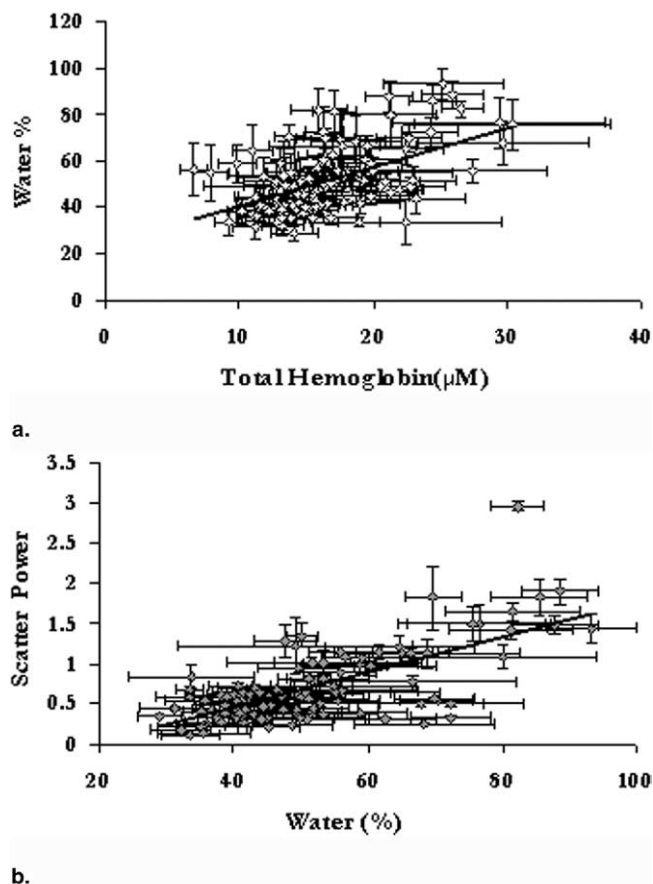


Figure 4. (a) Water versus total hemoglobin and (b) scatter power versus water. Both relationships have statistically significant correlations, with *P* < .001.

study (22) that indicated that whole breast values may not change significantly with different phases of the cycle, with changes possibly being limited to fibroglandular tissue volumes; in addition, our subject age group (age, 41–79 years; mean, 57 years) contains mostly subjects postmenopause or close to menopause. A younger population may show a stronger dependence on menstrual cycle (23,24).

Among the statistically significant correlations between demographic factors and NIR functional parameters, Hb_T related inversely with BMI (*P* < .001), consistent with earlier studies by our group, as well as by other researchers (19,22,25–27). BMI is indicative of the fat content of the breast; hence, greater values are associated with women whose breasts are composed predominantly of adipose tissue, which has lower vascularity (compared with glandular composition). Figure 1a, which shows this relationship, indicates that as BMI decreases (<25 kg/m²), the change in Hb_T is appreciable because of increased vascularity. However, as BMI increases to greater than 25 kg/m², a minimum value for Hb_T is reached based on physiological processes, beyond which an increase in BMI may have no effect on the vascularity. The inverse relationship between water and adipose tissue is well known; thus, the inverse correlation between water content and BMI is consistent with expectations. Water also correlated with age (*P* < .001). Cerussi et al (28,29) and Spinelli et al (27) showed indications of this relationship. In addition, age was shown to affect proliferative activity of the breast (30), and postmenopausal women were found to have lower water content than premenopausal women (23). Hence, the correlation between water content and age agrees with expected physiology and also highlights the importance of the improvement in water information with our new algorithm because these correlations were not significant in the previous data set (8).

Scatter amplitude and power show more independence in the analysis using the spectrally constrained reconstruction. Previously, both scatter amplitude and power correlated with breast diameter and separated the radiographic density categories. In the new data set, scatter amplitude correlated with breast diameter (*P* < .001), but not radiographic density, whereas scatter

power correlated with age ($P = .005$), as well as yields a separation between differing density categories. In previous studies (14,15), images produced with the spectral approach illustrated that scatter power was more indicative of bulk tissue composition. The trend in Figure 3a supports this hypothesis. Recently, Simick et al (30) showed that NIR spectroscopy has the potential to determine breast density with accuracy up to 90% when the parenchymal density pattern from mammograms (30) is used as the gold standard. Because breast density is related to risk for cancer (31,32), as well as decreased mammographic sensitivity (33), NIR offers an opportunity to noninvasively characterize breast composition and thereby stratify risk without ionizing radiation exposure. Because denser breasts have greater percentages of fibroglandular tissue; water also is expected to increase with density, as suggested in Figure 3b. Finally, the correlation between water and total hemoglobin shows that the greater vascularity found in fibroglandular breast tissues also tends to have greater water content. Water correlated with scatter power, probably for similar reasons, namely that fibroglandular tissue has greater scattering properties than adipose tissue.

It should be noted that the changes observed here likely are associated with volume fraction changes, rather than actual compositional alterations in the adipose and fibroglandular tissue (33). That is, changes observed in the NIR total breast averages resulting from increases in age and BMI reflect alterations in the compositional partitioning of the breast into adipose, vascular, and fibroglandular compartments.

In conclusion, results presented here represent a significantly expanded and more accurate assessment of NIR imaging parameters in healthy breasts. Importantly, prior trends observed in Hb_T relative to BMI and scattering relative to breast density remain intact and have been strengthened statistically. However, new associations between water percentage and BMI, as well as age, and more refined relationships between scattering amplitude and scattering power with respect to breast diameter and radiodensity classification are now evident in statistically valid correlations. The observed trends are consistent with physiological expectations related to the aging process and known characteristics of breast parenchymal patterns. Their appearance in the current analysis is attributed to the improved accuracy available through direct spectral reconstruction. Changes found in total breast average NIR properties most likely are a reflection of

variations in compositional partitioning of the breast and not fundamental changes in NIR characteristics of an individual compartment such as fat.

REFERENCES

1. Ntzachristos V, Chance B. Probing physiology and molecular function using optical imaging: applications to breast cancer. *Breast Cancer Res* 2001; 3:41–46.
2. Fantini S, Moesta KT, Pogue BW. Optics in breast cancer. *J Biomed Opt* 2004; 9(6):1121.
3. Jobsis FF. Non-invasive, infra-red monitoring of cerebral and myocardial oxygen sufficiency and circulatory parameters. *Science* 1977; 198(4323): 1264–1267.
4. Boulnois J-L. Photophysical processes in recent medical laser developments: a review. *Lasers Med Sci* 1986; 1:47–66.
5. Mourant JR, Fuselier T, Boyer J, Johnson TM, Bigio IJ. Predictions and measurements of scattering and absorption over broad wavelength ranges in tissue phantoms. *Appl Opt* 1997; 36:949–957.
6. van Staveren HJ, Moes CJM, van Marle J, Prahl SA, van Gemert JC. Light scattering in intralipid-10% in the wavelength range of 400–1100 nm. *Appl Opt* 1991; 30:4507–4514.
7. Thomsen S, Tatman D. Physiological and pathological factors of human breast disease that can influence optical diagnosis. *Ann N Y Acad Sci* 1998; 838:171–193.
8. Srinivasan S, Pogue BW, Jiang S, et al. Interpreting hemoglobin and water concentration, oxygen saturation and scattering measured in vivo by near-infrared breast tomography. *PNAS* 2003; 100:12349–12354.
9. Corlu A, Durduran T, Choe R, et al. Uniqueness and wavelength optimization in continuous-wave multispectral diffuse optical tomography. *Opt Lett* 2003; 28:2339–2341.
10. Li A, Zhang Q, Culver JP, Miller EL, Boas DA. Reconstructing chromosphere concentration images directly by continuous-wave diffuse optical tomography. *Opt Lett* 2004; 29:256–258.
11. Srinivasan S, Pogue BW, Jiang S, Dehghani H, Paulsen KD. Spectrally constrained chromophore and scattering NIR tomography provides quantitative and robust reconstruction. *Appl Opt* 2005; 44:1858–1869.
12. Li A, Boverman G, Zhang Y, et al. Optimal linear inverse solution with multiple priors in diffuse optical tomography. *Appl Opt* 2005; 44:1948–1956.
13. Brooksby B, Srinivasan S, Jiang S, Dehghani H, Pogue BW, Paulsen KD. Spectral-prior information improves near-infrared diffuse tomography more than spatial-prior. *Opt Lett* 2005; 30(15):1968–1970.
14. Srinivasan S, Pogue BW, Brooksby B, et al. Near-infrared characterization of breast tumors in-vivo using spectrally-constrained reconstruction. *Technol Cancer Res Treatment* 2005; 4:513–526.
15. Jakubowski DB, Cerussi AE, Bevilacqua F, et al. Monitoring neoadjuvant chemotherapy in breast cancer using quantitative diffuse optical spectroscopy: a case study. *J Biomed Opt* 2004; 9:230–238.
16. Shah N, Cerussi A, Jakubowski D, Hsiang D, Butler J, Tromberg B. The role of diffuse optical spectroscopy in the clinical management of breast cancer. *Dis Markers* 2003–2004; 19:95–105.
17. McBride TO, Pogue BW, Jiang S, Osterberg UL, Paulsen KD. A parallel-detection frequency-domain near-infrared tomography system for hemoglobin imaging of the breast in vivo. *Rev Sci Instruments*, 2001; 72: 1817–1824.
18. Paulsen KD, Jiang H. Spatially varying optical property reconstruction using a finite element diffusion equation approximation. *Med Phys* 1995; 22:691–701.
19. Poplack SP, Paulsen KD, Hartov A, et al. Electromagnetic breast imaging: average tissue property values in women with negative clinical findings. *Radiology* 2004; 231:571–580.
20. ACR. Breast Imaging Reporting and Data System (BIRADS™). Reston, VA: American College of Radiology, 1998.
21. Quaresima V, Matcher SJ, Ferrari M. Identification and quantification of intrinsic optical contrast for near-infrared mammography. *Photochem Photobiol* 1998; 67:4–14.

22. Pogue BW, Jiang S, Dehghani H, et al. Characterization of hemoglobin, water and NIR scattering in breast tissue: analysis of inter-subject variability and menstrual cycle changes relative to lesions. *J Biomed Opt* 2004; 9:541–552.
23. Shah N, Cerussi A, Eker C, et al. Noninvasive functional optical spectroscopy of human breast tissue. *Proc Natl Acad Sci U S A* 2001; 98:4420–4425.
24. Cubeddu R, D'Andrea C, Pifferi A, Taroni P, Torricelli A, Valentini G. Effects of the menstrual cycle on the red and near-infrared optical properties of the human breast. *Photochem Photobiol* 2000; 72:383–391.
25. Durduran T, Choe R, Culver JP, et al. Bulk optical properties of healthy female breast tissue. *Phys Med Biol* 2002; 47:2847–2861.
26. Intes X, Djeziri S, Ichlalene Z, et al. Time-Domain Optical Mammography SoftScan: initial results. *Acad Radiol* 2005; 12:934–947.
27. Spinelli L, Torricelli A, Pifferi A, Taroni P, Danesini GM, Cubeddu R. Bulk optical properties and tissue components in the female breast from multiwavelength time-resolved optical mammography. *J Biomed Opt* 2004; 9:1137–1142.
28. Cerussi A, Jakubowski D, Shah N, et al. Spectroscopy enhances the information content of optical mammography. *J Biomed Opt* 2002; 7:60–71.
29. Potten CS, Watson RJ, Williams GT, et al. The effect of age and menstrual cycle upon the proliferative activity of the normal human breast. *Br J Cancer* 1988; 58:163–170.
30. Simick MK, Jong R, Wilson B, Lilge L. Non-ionizing near-infrared radiation transillumination spectroscopy for breast tissue density and assessment of breast cancer risk. *J Biomed Opt* 2004; 9:794–803.
31. Mandelson MT, Oestreicher N, Porter PL, et al. Breast density as a predictor of mammographic detection: comparison of interval- and screen-detected cancers. *J Natl Cancer Inst* 2000; 92:1081–1087.
32. Buist DSM, Porter PL, Lehman C, Taplin SH, White E. Factors contributing to mammography failure in women aged 40–49 years. *J Natl Cancer Inst* 2004; 96:1432–1440.
33. Brooksby B, Pogue BW, Jiang S, et al. Hybrid breast imaging: near infrared spectral tomography and MRI. *Nat Biotechnol* Submitted 2005; Manuscript in submission.